Supplementary Information for

Dependence of Reactive Oxygen Species Formation on Oxidation State of Biogenic Secondary Organic Aerosols

Kasey C. Edwards,[1] Lena Gerritz,[1] Meredith Schervish,[1] Manjula Canagaratna,[2] Anita M. Avery,[2] Mitchell W. Alton,[2] Lisa M. Wingen,[1] Jackson T. Ryan,[1] Celia Faiola,[1] Andrew T. Lambe,[2] Sergey A. Nizkorodov,[1] Manabu Shiraiwa[1*]

[1] Department of Chemistry, University of California, Irvine, Irvine, CA, 92697, United States

[2] Center for Aerosol and Cloud Chemistry, Aerodyne Research Inc., Billerica, MA, 01821, United States

*m.shiraiwa@uci.edu

Contents of this file
Pages: 8
Figures: 9

Text S1. ROOH Yield Simulation Using the Radical 2D-VBS Model

The radical 2D-volatility basis set model (r2D-VBS) has been described in detail in previous work but a brief discussion is given here.[1-3] This model simulates gas-phase chemistry through representative peroxy radical (RO_2) species and ultimately distributes these products into the 2D-VBS based on volatility or effective saturation mass concentration (C^*) using semiempirical kernels for each radical termination reaction. Because specific functional group information about the oxidized SOA is unknown, we made assumptions about the −OOH groups present on the molecules. Since autoxidation leads to organic hydroperoxide (ROOH) formation, we counted every step of autoxidation a molecule has undergone as being an additional −OOH group that can decompose. Products from the $RO_2^\bullet + HO_2^\bullet$ reaction were included as this termination reaction will produce ROOH, however dimerization products of the $RO_2^\bullet + RO_2^\bullet$ reaction were not included unless they underwent autoxidation. The -OOH yield was calculated as the number of -OOH groups formed in VBS bins that contributed to the particle phase divided by the total carbon in VBS bins that contribute to the particle phase.

For this work, we run the model with a constant flow of d-limonene and with a range of $^\bullet$OH from 0.1-10 × 10^8 cm^{-3}. The radical 2D-VBS does not include any dynamic gas-particle partitioning. To estimate the ROOH concentration in the particle phase, we only included VBS bins which contribute to particles when 325 μg m^{-3} of organic aerosol is present (this specific value was chosen as it was the most often observed OA concentration in the OFR). This leads to ~3/4 of the C^* = 100 μg m^{-3} bin and ~1/4 of the C^* = 1000 μg m^{-3} bin being included. All molecules in bins with $C^* < 100$ μg m^{-3} were included, and none were included from bins with $C^* > 1000$ μg m^{-3}. ROOH fragmentation is not considered in the model.

Figure S7 shows 2D-VBS modeling results of -OOH yield as a function of [OH] and [OHexp], which signify increased oxidative aging time for d-limonene SOA. The decrease of -OOH yield is consistent with peroxide measurements, in which higher O/C leads to a decrease in -OOH yield. Note that the absolute amount of ROOH in the particles (and the concentration of ROOH being formed in the gas phase) increases, while the -OOH yield decreases. The model does not consider HO_2 formation from OH oxidation of terpenes, therefore hydroperoxide formation may be underpredicted. On the other hand, neither fragmentation nor multigeneration products of OH oxidation of SOA are considered, which are likely common in the flow tube with a substantially high concentration of $^\bullet$OH. As opposed to autoxidation which favors ROOH functionality,[4, 5] multigenerational $^\bullet$OH oxidation could lead to a higher concentration of different functionality, reducing the overall contribution from ROOH.[6]

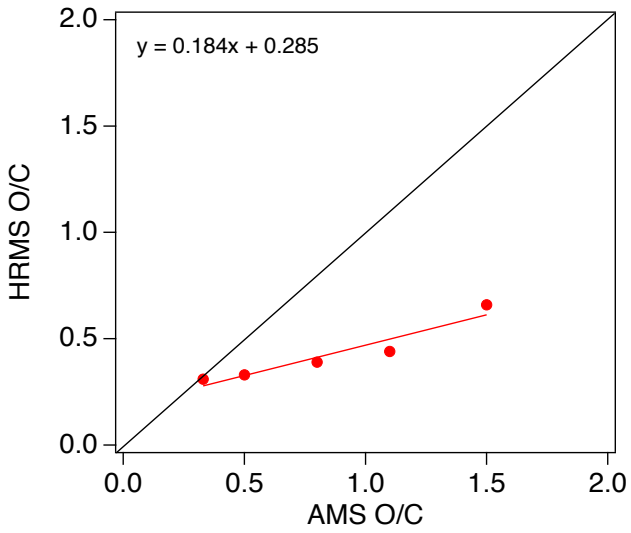

Figure S1: Comparison of O/C values from AMS (X-axis) and HRMS (Y-axis). Values are taken from filter analysis of both d-limonene SOA and β-caryophyllene SOA.

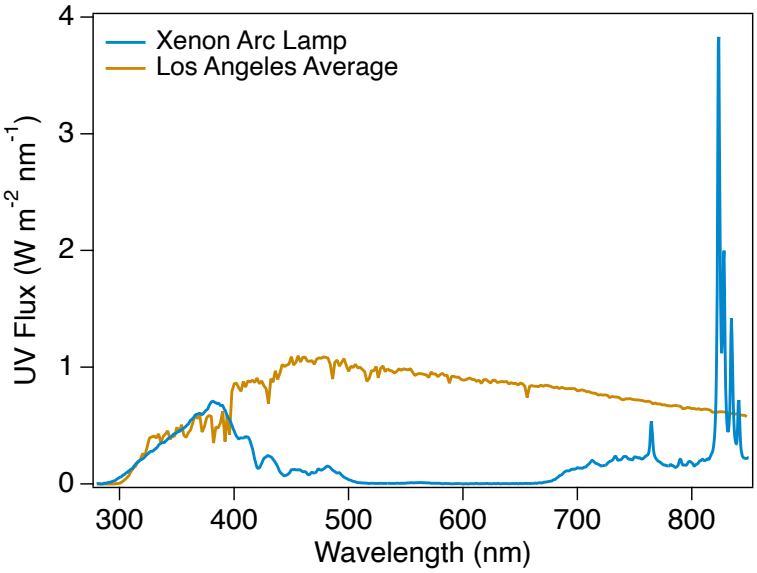

Figure S2: Spectral flux density (W m^{-2} nm^{-1}) from the Xenon Arc lamp used in photoirradiation experiments compared with Los Angeles solar flux daily average for June 20. The visible portion of the Xe-lamp spectrum is filtered out with a combination of filters to minimize heating of the irradiated filter.

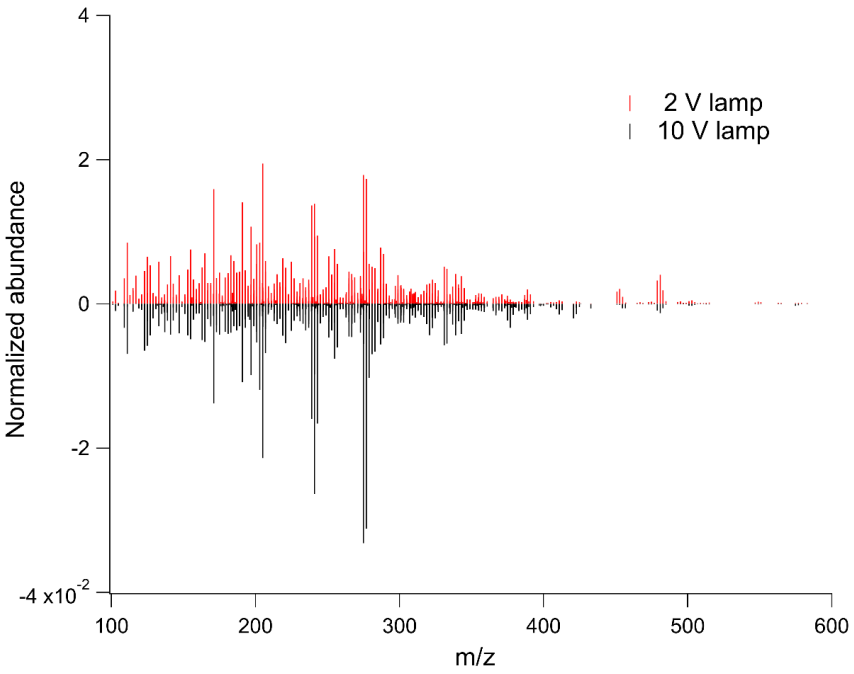

Figure S3: Mass spectrum of limonene SOA produced from Cl oxidation at lamp intensities of 2 V (red) and 10 V (gray) measured using negative ion mode HRMS.

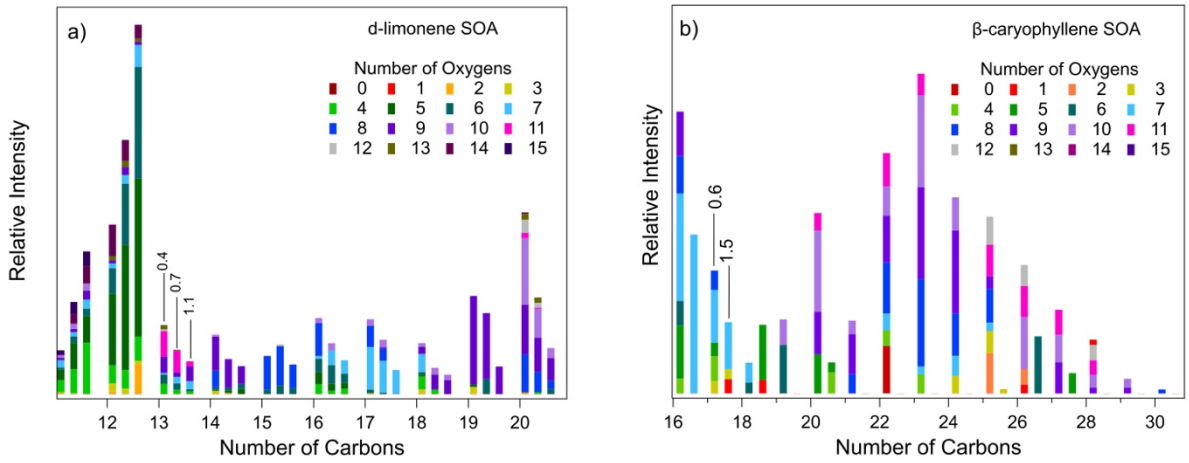

Figure S4: Carbon number with associated oxygen number of d-limonene SOA (a) and β-caryophyllene SOA (b). This figure expands the portion of Figure 2 to better illustrate what happens for c>10 compounds for d-limonene and c>15 compounds for β-caryophyllene. Samples of low O/C are shown on the left and high O/C samples are shown on the right. Mid-level O/C samples are shown in the middle for d-limonene SOA.

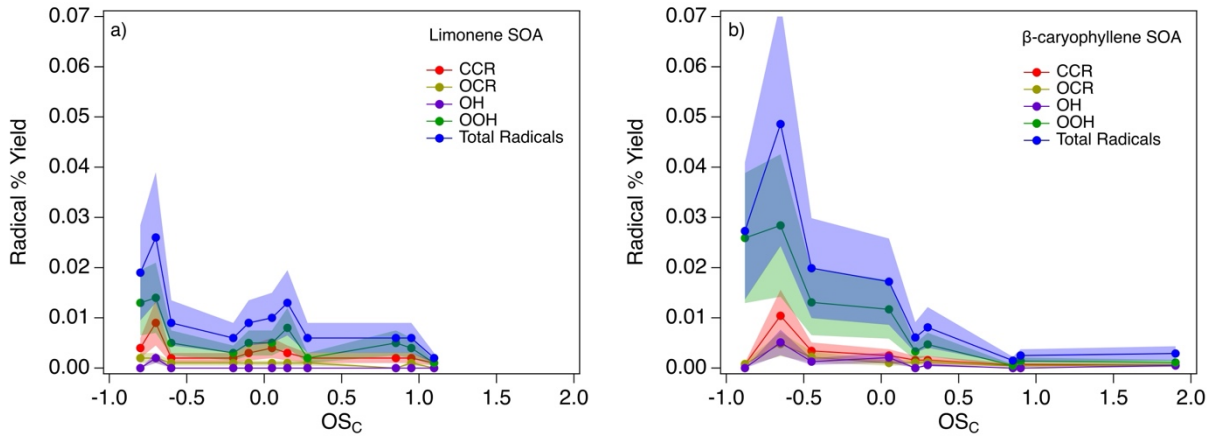

Figure S5: Radical % yield vs OS_C for d-limonene SOA (a) and β-caryophyllene SOA (b). Shaded regions represent error bars equalling 50% of the measured y-value including error from mass and ROS meaursements. The oxidation state of carbon (OS_C), a useful metric for determining the degree of oxidation for SOA, differs from O/C in that it is independent of hydration and dehdration of an aerosol, and can properly account for oxidation that does not result in a change of O/C, such as an alcohol oxidation to a cabonyl.[7, 8]

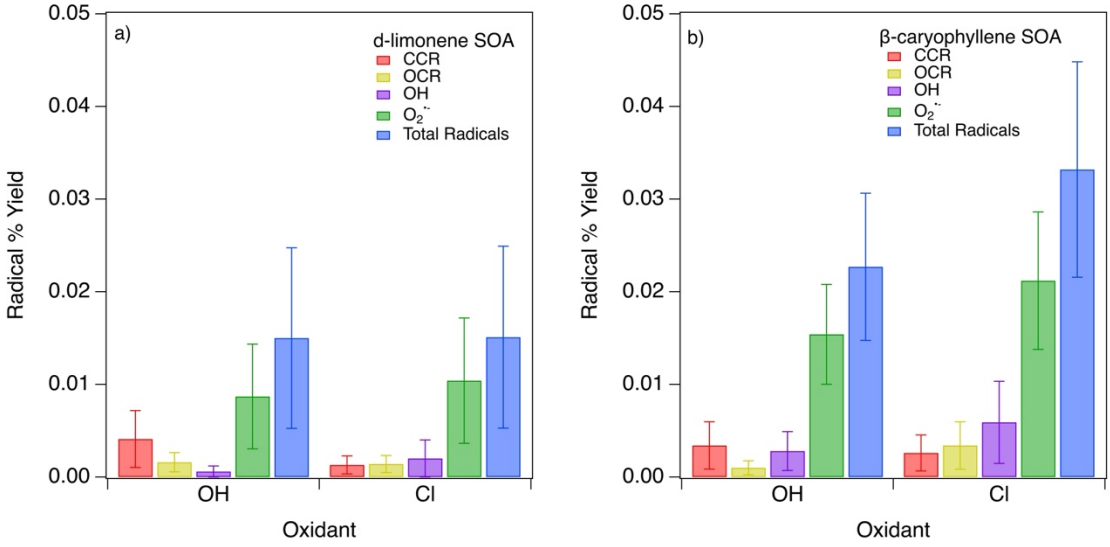

Figure S6: Radical % yield of d-limonene SOA (a) and β-caryophyllene SOA (b) using either •Cl or •OH as the oxidant in the OFR. D-limonene SOA are compared with O/C = 0.5±0.1 for both •OH and •Cl samples. β-caryophyllene SOA are compared with O/C = 0.6±0.1 for both •OH and •Cl samples. Error is taken as the standard deviation of three replicates.

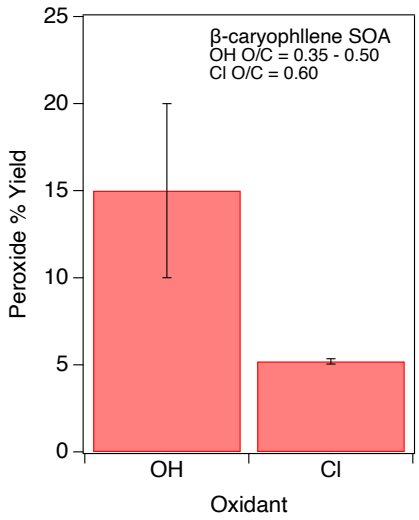

Figure S7: Peroxide % yield from β-caryophyllene SOA generated with Cl as the oxidant. Cl-SOA shows 10% lower peroxide formation than OH-SOA. Lower peroxide yield from Cl-SOA is expected due to lower HO_2 generation in the •Cl chamber, reducing the $RO_2 + HO_2$ reaction rate, and therefore ROOH production. One additional reason for less peroxide content observed with •Cl is due to the higher O/C of the •Cl sample compared to the •OH oxidized sample.

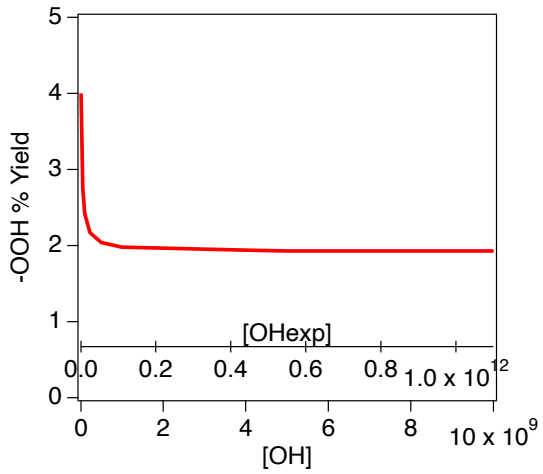

Figure S8: 2D-VBS modeling results of -OOH yield as a function of [OH] and [OHexp] are shown, which signify increased oxidative aging time for d-limonene SOA. These results support our peroxide measurements, in which further oxidation or higher O/C leads to a decrease in -OOH yield.

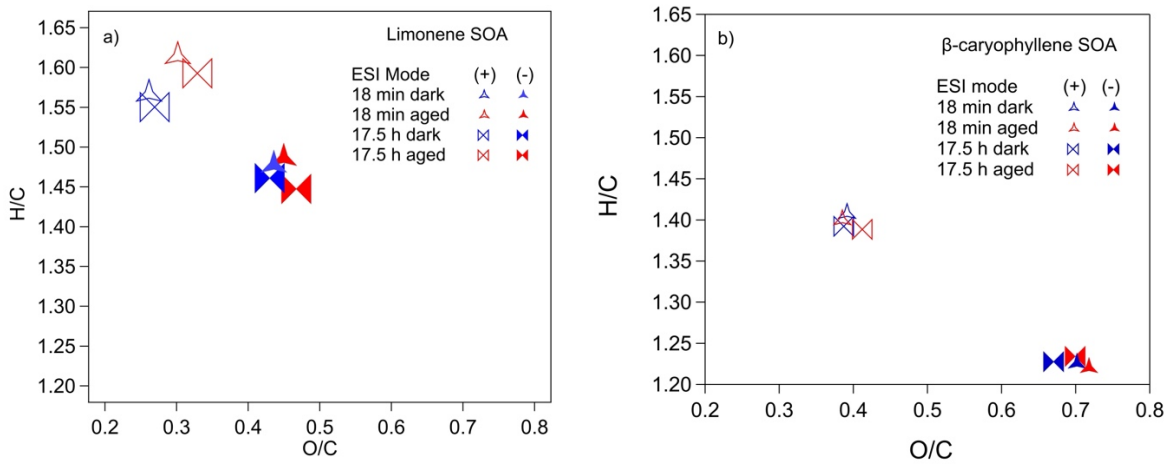

Figure S9: O/C and H/C shift with photolytic aging for d-limonene SOA (a) and β-caryophyllene SOA (b) in positive and negative ion mode. Minor changes in O/C and H/C were observed with photolytic aging up to 17.5 hours. HRMS O/C values are underestimated due to selective ionization as shown in Figure S1, so future studies may be warranted to confirm changes in O/C with photoaging.

References:

(1) Schervish, M.; Donahue, N. M. Peroxy radical kinetics and new particle formation. *Enviiron. Sci. Atmos.* **2021**, *1* (2), 79-92.
(2) Schervish, M.; Donahue, N. M. Peroxy radical chemistry and the volatility basis set. *Atmospheric Chemistry and Physics* **2020**, *20* (2), 1183-1199.
(3) Schervish, M.; Heinritzi, M.; Stolzenburg, D.; Dada, L.; Wang, M. Y.; Ye, Q.; Hofbauer, V.; Devivo, J.; Bianchi, F.; Brilke, S.; Duplissy, J.; El Haddad, I.; Finkenzeller, H.; He, X. C.; Kvashnin, A.; Kim, C.; Kirkby, J.; Kulmala, M.; Lehtipalo, K.; Lopez, B.; Makhmutov, V.; Mentler, B.; Molteni, U.; Nie, W.; Petäjä, T.; Quéléver, L.; Volkamer, R.; Wagner, A. C.; Winkler, P.; Yan, C.; Donahue, N. M. Interactions of peroxy radicals from monoterpene and isoprene oxidation simulated in the radical volatility basis set. *Environ Sci-Atmos* **2024**, *4* (7), 740-753.
(4) Bianchi, F.; Kurtén, T.; Riva, M.; Mohr, C.; Rissanen, M. P.; Roldin, P.; Berndt, T.; Crounse, J. D.; Wennberg, P. O.; Mentel, T. F.; Wildt, J.; Junninen, H.; Jokinen, T.; Kulmala, M.; Worsnop, D. R.; Thornton, J. A.; Donahue, N.; Kjaergaard, H. G.; Ehn, M. Highly Oxygenated Organic Molecules (HOM) from Gas-Phase Autoxidation Involving Peroxy Radicals: A Key Contributor to Atmospheric Aerosol. *Chem. Rev.* **2019**, *119* (6), 3472-3509.
(5) Crounse, J. D.; Nielsen, L. B.; Jørgensen, S.; Kjaergaard, H. G.; Wennberg, P. O. Autoxidation of organic compounds in the atmosphere. *The Journal of Physical Chemistry Letters* **2013**, *4* (20), 3513-3520.
(6) Wang, M. Y.; Chen, D. X.; Xiao, M.; Ye, Q.; Stolzenburg, D.; Hofbauer, V.; Ye, P. L.; Vogel, A. L.; Mauldin, R. L.; Amorim, A.; Baccarini, A.; Baumgartner, B.; Brilke, S.; Dada, L.; Dias, A.; Duplissy, J.; Finkenzeller, H.; Garmash, O.; He, X. C.; Hoyle, C. R.; Kim, C.; Kvashnin, A.; Lehtipalo, K.; Fischer, L.; Molteni, U.; Petäjä, T.; Pospisilova, V.; Quéléver, L. L. J.; Rissanen, M.; Simon, M.; Tauber, C.; Tomé, A.; Wagner, A. C.; Weitz, L.; Volkamer, R.; Winkler, P. M.; Kirkby, J.; Worsnop, D. R.; Kulmala, M.; Baltensperger, U.; Dommen, J.; El Haddad, I.; Donahue, N. M. Photo-oxidation of Aromatic Hydrocarbons Produces Low-Volatility Organic Compounds. *Environmental Science & Technology* **2020**, *54* (13), 7911-7921.
(7) Canagaratna, M. R.; Jimenez, J. L.; Kroll, J. H.; Chen, Q.; Kessler, S. H.; Massoli, P.; Hildebrandt Ruiz, L.; Fortner, E.; Williams, L. R.; Wilson, K. R.; Surratt, J. D.; Donahue, N. M.; Jayne, J. T.; Worsnop, D. R. Elemental ratio measurements of organic compounds using aerosol mass spectrometry: characterization, improved calibration, and implications. *Atmospheric Chemistry and Physics* **2015**, *15* (1), 253-272.
(8) Kroll, J. H.; Donahue, N. M.; Jimenez, J. L.; Kessler, S. H.; Canagaratna, M. R.; Wilson, K. R.; Altieri, K. E.; Mazzoleni, L. R.; Wozniak, A. S.; Bluhm, H.; Mysak, E. R.; Smith, J. D.; Kolb, C. E.; Worsnop, D. R. Carbon oxidation state as a metric for describing the chemistry of atmospheric organic aerosol. *Nat Chem* **2011**, *3* (2), 133-139.